

**HIGH RESOLUTION INFRARED SPECTROSCOPY FROM SPACE: A PRELIMINARY REPORT
ON THE RESULTS OF THE ATMOSPHERIC TRACE MODULE SPECTROSCOPY (ATMOS)
EXPERIMENT ON SPACELAB 3**

Crofton B. Farmer and Odell F. Raper
Jet Propulsion Laboratory
California Institute of Technology

ABSTRACT

The ATMOS (Atmospheric Trace Molecule Spectroscopy) experiment has the broad purpose of investigating the physical structure, chemistry, and dynamics of the upper atmosphere through the study of the distributions of the neutral minor and trace constituents and their seasonal and long-term variations. The technique used is high-resolution infrared absorption spectroscopy using the Sun as the radiation source, observing the changes in the transmission of the atmosphere as the line-of-sight from the Sun to the spacecraft penetrates the atmosphere close to the Earth's limb at sunrise and sunset. During these periods, interferograms are generated at the rate of one each second which yield, when transformed, high resolution (0.01 cm^{-1}) spectra covering the 2.2 to 16 micron region of the infrared. Twenty such occultations were recorded during the Spacelab 3 flight, which have produced concentration profiles for a large number of minor and trace upper atmospheric species in both the northern and southern hemispheres. Several of these species have not previously been observed in spectroscopic data. The data reduction and analysis procedures used following the flight are discussed in the present paper; a number of examples of the spectra obtained are shown, and a bar graph of the species detected thus far in the analysis is given which shows the altitude ranges for which concentration profiles have been retrieved.

INTRODUCTION

Infrared absorption spectroscopy, using the Sun as the radiation source, has proven to be one of the most powerful methods for studying the composition and structure of the Earth's atmosphere. Such measurements can provide information on the vertical and spatial distribution of the molecular constituents of the atmosphere, the local temperature and pressure regimes, and the photochemical, thermodynamic, and radiative transfer processes which are occurring there. Studies of this kind were made in the past from the surface and from low-flying aircraft [1] and have progressed more recently to high-flying aircraft and balloons [2]. It has been apparent for some time that the next logical step in the utilization of spectroscopic techniques for atmospheric measurements is to make the observations from space. Such measurements afford the possibility of probing the entire altitude range of the atmosphere, and offer the additional advantage of providing global coverage. The Atmospheric Trace Molecule Spectroscopy (ATMOS) investigation was conceived and implemented to take advantage of the capabilities of the Space Transportation System (STS) which provides the space shuttle as a platform for making such measurements from space and the Tracking Data and Relay Satellite System (TDRSS) for relaying high data rate information to the ground.

THE ATMOS INSTRUMENT

Against the two obvious advantages of probing the upper atmosphere from space there lies the disadvantage of the very rapid rates at which the solar occultations occur while in Earth orbit. This disadvantage is compounded by the fact that there are more than 40 atmospheric molecular species of

interest today which absorb at a wide range of frequencies in the near and middle infrared, making broad wavelength coverage at very fast scan rates a necessity. The only technique capable of acquiring spectra under such conditions is fast Fourier Transform (FFT) spectroscopy; this consideration established the requirements for the sensor (a state-of-the-art Michelson interferometer) to be used in the investigation.

The ATMOS instrument, described in Reference 4 and illustrated in Figure 1, was designed and built by Honeywell Electro-Optics Center (HEOC) in Wilmington, Massachusetts; an optical diagram tracing the radiation path through the instrument is shown in Figure 2. The salient characteristics of the instrument, dictated by the demanding task of acquiring broad band, high resolution spectra from space, are listed in Table 1. The one-second scan time shown in the table is based on the need for good vertical resolution in the measurements and the assumption of a worst-case occultation rate of 2.5 km per second. In order to reduce the sampling rate and improve the signal-to-noise characteristics of the spectra, the overall spectral range of interest, from 550 to 4800 cm^{-1} , is divided into four smaller, overlapping wavelength intervals using optical filters whose bandpasses fit within the alias limits created by sampling every two or every three fringes of the He-Ne reference laser. The wavelength intervals covered by these filters, together with those molecules of interest having absorption features which fall within each region, are shown in Table 2. Not shown in the table are two additional filters including a notch filter (No. 5) covering the regions from 600 to 700 cm^{-1} and from 2000 to 2500 cm^{-1} (used for temperature sounding and thermodynamic equilibrium studies), and a broad survey filter (No. 6) which covers the entire spectral region from 600 to 3600 cm^{-1} with reduced signal-to-noise performance.

MISSION PROFILE

The Spacelab 3 mission was flown by the space shuttle Challenger during the period from April 29, 1985, to May 6, 1985. The launch time for the mission was chosen by the ATMOS Science Team such that sunset occultations during the flight would occur in a broad band of northern latitudes encompassing the region from 10° to 40°N, and sunsets in the southern latitude band from 40° to 50°S. Over 50 sunset and sunrise occultations had been allocated to ATMOS to fulfill the primary objective of detecting as many as possible of the minor and trace species present in the upper atmosphere and determining their vertical distributions, and the secondary objectives as well as discerning their latitudinal and longitudinal distributions. The use of the optical filters available in the instrument was planned such that good sampling of the latitudinal and longitudinal distributions of each of the species could be obtained.

Very early in the mission, engineering telemetry data from the instrument indicated a leak in a pressurized housing which contained the He-Ne reference laser. This information forewarned that the housing would eventually reach a pressure low enough to cause arcing in the high voltage power supply for the laser. Prior to the shutdown of the instrument 20 sunset and sunrise occultations were obtained. This number of occultations was completely sufficient to satisfy the primary objectives of the flight; a summary listing of these occultations and their geographical locations is shown in Table 3. In all, the total raw data returned during the abbreviated mission amounted to about 9 gigabytes.

DATA REDUCTION

One of the marked disadvantages of interferometric spectroscopy, at least until recent times, has been the amount of processing required on the raw data contained in the interferograms. Because of the large dynamic range of the data in an interferogram, most interferometers contain both a high and a low gain data channel and these must be merged into one data stream at the beginning of the reduction period. Corrections for phase distortion must be applied to a subset of the interferogram points in the

region of the zero path difference fringe, and finally the entire set of interferogram points must be Fourier-transformed from interferometric space to spectral space in order to provide data records suitable for examination. Not until the evolution of modern computers and array processors, with their large throughput capacities and ultra-high operational speeds, did large scale measurements with high resolution Fourier transform spectrometers become a viable technique. In the case of ATMOS, a dedicated facility was constituted at JPL to accomplish the formidable data reduction and analysis tasks. At the core of this facility are a powerful minicomputer and two fast array processors which can – in a matter of seconds – perform the phase correction and Fourier transformation required to convert a 400,000 point, 16 megabit ATMOS interferogram into a spectrum.

During the Spacelab 3 mission, 3 minutes' worth of data were gathered by the instrument at each occultation opportunity. Since the occultation rates on Spacelab 3 were of the order of 2 km/sec, more than half of the spectra in each occultation set were solar, i.e., were acquired above the Earth's atmosphere and contained features of solar origin only. In order to simplify the analysis task on the atmospheric spectra, a number of the solar-only spectra were averaged together for each of the occultations and the resultant spectrum was ratioed against each of the spectra in the set which contained telluric features, effectively removing all of the superimposed solar lines from each spectrum. At a later date, more comprehensive averages of the solar spectra available from the mission will be assembled and the results published as a high signal-to-noise, high resolution solar atlas covering the infrared wavelength region from 2.2 to 16 microns.

DATA ANALYSIS

There are two major phases involved in that part of the analysis of the data leading to profiles of concentration for the minor and trace gases. While initially both may be pursued simultaneously on an iterative basis, the accuracies achieved in the first phase, which involves the extraction of temperature and pressure information from the spectra for each occultation, ultimately establishes the uncertainties associated with the retrieval of the mixing ratio profiles themselves (which constitutes the second phase). In view of this, one of the advantages of the wide spectral coverage and high resolution of the data is the convenient access to spectral features that can be used for determining the vertical profile of pressure and temperature corresponding to each occultation location. Of particular importance in this context are the lines of the 1-0 N_2 quadrupole band that occur between CO_2 ν_3 band head and the $\nu_1 + 2\nu_2$ band of N_2O . A number of these lines can be seen in the lower trace of Figure 3. The S8 and S10 lines of N_2 at 2403.6 and 2418.7 are essentially insensitive to temperature (having lower state energies of 143.2 cm^{-1} and 218.8 cm^{-1} , respectively), and their strengths give lines of convenient intensity at this resolution for quantitative analysis of tangent heights from the tropopause to about 35 km, which is the range over which refraction coupled with increasing atmospheric opacity result in nonuniform spacing of the tangent altitudes of successive scans. They thus provide an ideal means for the determination of the line-of-sight column density corresponding to each scan. Furthermore, since ray paths with tangent altitudes of between 15 and 30 km correspond to air-mass values between 10 and 1, respectively, the N_2 lines can be carefully "calibrated" by reference to spectral scans made by the instrument observing the Sun from the ground. Together with the temperature sensitive (high-J) CO_2 lines, these features provide the basis for inverse methods for the retrieval of temperature-pressure profiles. In the 30 to 40 km range numerous temperature insensitive CO_2 lines can be utilized for the determination of the line-of-sight column density; by comparison of these with the N_2 lines in the same spectra, systematic uncertainties in the molecular spectral parameters of the CO_2 bands can be minimized. In this way the range over which reliable temperature profile retrievals are possible can be extended upwards well into the mesosphere, to altitudes where the effects of photolysis of CO_2 and departure from local thermodynamic equilibrium negate many of the assumptions that can be made at lower altitudes in comparing the observed spectra with the results expected from the application of simple radiative transfer

theory. Figure 4 shows an example of two retrievals to determine the pressure-temperature profiles corresponding to two of the ATMOS Spacelab 3 occultations.

At the time of writing, most of the effort in determining the atmospheric temperature, pressure, and density structure at the occultation locations has been concentrated on analyses in the 4 and 2.7 micron regions (i.e., the data obtained with filter 3), mainly for reasons related to the quality of the laboratory spectral data available in these bands. It was anticipated prior to the Spacelab 3 flight that this would be the case, and filter 3 occultations were scheduled with sufficient frequency such that temperature and pressure data derived from them could reasonably be extrapolated to the occultations utilizing other filters recorded in the near (geographical) vicinity.

The approach adopted for deriving the profiles of concentration from the data was to preselect very narrow wavelength regions in the spectra which contain analyzable features of each gas of interest, and to manipulate these "microwindows" rather than the huge spectral sets themselves. To give an indication of the quality of the data and to illustrate the remarkable power of the Fourier transform technique when used in this way, the top trace in Figure 5 shows a segment of about 500 cm^{-1} from one of the Filter 2 observations. The succeeding traces show the same data at successively higher dispersions by factors of ~ 10 and finally ending with a 1.0 cm^{-1} segment centered at 915 cm^{-1} , which corresponds to one of the selected microwindows for NO. Figure 6 shows the entire set of spectra in this microwindow region for this occultation and the windows depicted in both Figure 5 and Figure 6 are non-ratioed tracings showing the very different growth characteristics between the NO lines and the water vapor lines identified in the figures, and the constant absorption characteristics of solar features. Suitable microwindow regions were selected prior to the Spacelab 3 flight by the ATMOS Science Team members using the best distribution estimates available at the time for each molecule, a standard physical model of the atmosphere, and synthetic spectra generated with the aid of a 150-layer model atmosphere program. To analyze the actual flight spectra, a program was created which automatically extracts from the data the microwindows specified by the user and displays them — three successive spectra at a time — on the computer terminal screen. Starting at the highest altitude desired, the user can then activate automatic features of the program which create and iterate synthetic spectra to fit the spectral features contained in the microwindow and proceed downward (in tangent altitude) in "onion peel" fashion until a concentration profile for the species of interest as a function of altitude is derived. In general, several microwindows are used to derive separate profiles for a given species in each occultation, the individual profiles then being averaged to improve the accuracy of the final result.

Because of the magnitude of the spectral data sets which can be obtained from an instrument of this type, a large body of additional software has been written to facilitate the ATMOS data analysis activities, including programs for displaying and manipulating real and synthetic spectra, the atmospheric physical and chemical models, and the contents of the ATMOS library of molecular spectral parameters (the "ATMOS linelist"). Both on-line and off-line plotting programs and devices are also available for hardcopy graphical presentations of the data. All of the spectral examples shown in this report were reproduced directly from the output of these peripheral devices.

RESULTS

Representative examples of the ATMOS spectra illustrating the quality of the data and a few of the many interesting spectral features observed are shown in Figures 7 through 11. Figure 12 is a diagrammatic summary indicating the vertical range of detection for those species whose profiles have been extracted from the data at this stage of the analysis. Notable among the results are the detection of several trace species that had not been observed previously (namely COF_2 , N_2O_5 , and HNO_4), the

confirmation of the presence of ClONO_2 in the stratosphere through the identification of 5 separate vibration-rotation bands, and the first measurement by remote sensing techniques of the principal natural halocarbon, CH_3Cl . As can be seen in Figure 12, the resolution and sensitivity of the ATMOS instrument is sufficient to allow continuous profiles of concentration for some minor gases (and at least one trace gas) to be determined extending from the upper troposphere through the stratosphere and mesosphere and, in the case of CO_2 , CO , and NO well into the lower thermosphere (i.e., ~ 130 km). However, the derivation of the profiles in the mesosphere is complicated by the fact that the onset of photochemical thresholds for dissociation and the potential departure from thermodynamic and equilibrium conditions in these regions render invalid many of the assumptions which can be made at lower altitudes to help in establishing the temperature and pressure environment for the species being measured. It is the task of the ATMOS Science Team over the next several months to unravel the radiative transfer, thermodynamic, photochemical, and transport processes which are occurring in these regions and improve our understanding of the physical conditions at these hitherto uncharted altitudes in our atmosphere.

FUTURE MISSIONS

While the ATMOS flight on Spacelab 3 was conducted in accordance with a comprehensive set of scientific objectives, it can also be viewed as a "proof of concept" flight which validated the instrument and experimental techniques to be used for the long range objectives of the ATMOS Investigation. ATMOS will be a core part of the Earth Observations Missions (EOM) beginning in August of 1986 and continuing for a period of at least an eleven-year solar cycle with about one flight per year. Short range objectives for these missions are expected to be planned on the basis of the current status of upper atmospheric knowledge and the flight conditions for the individual mission opportunities as they arise. The opportunity will be taken to make flights at different seasons and inclinations in order to provide the required range of observational parameters for discerning latitudinal and seasonal changes in the upper atmospheric inventory of molecular species. The data from Spacelab 3 will provide an archival record against which the results from later flights can be compared to study any long term changes in the composition of the atmosphere.

ACKNOWLEDGMENTS

The authors wish to thank the ATMOS coinvestigators and their colleagues for making available the results of work in progress which have contributed to this preliminary report. We are also grateful to Leslie Lowes, Susan Paradise, and Margaret Dietrich for their help in preparing the manuscript. We are deeply indebted to Joe Cremin, the Spacelab 3 Mission Manager, and the entire Payload Operations Control Center (POCC) cadre team for rising to the occasion when informed of the laser housing problem with ATMOS and rescheduling timed events to move as many as possible of the ATMOS occultations to earlier times in the mission, thus preserving the primary objectives of the investigation.

The research described in this paper was performed by the Jet Propulsion Laboratory, California Institute of Technology, under contract with NASA.

REFERENCES

1. Farmer, C. B.: Infrared Measurements of Stratospheric Composition. *Can. J. Chem.*, Vol. 52, 1974, pp. 1544-1559.
2. Farmer, C. B., Raper, O. F., and Norton, R. H.: Spectroscopic Detection and Vertical Distribution of HCl in the Troposphere and Stratosphere. *Geophys. Res. Lett.*, Vol. 3, 1976, pp. 13-16.
3. Farmer, C. B., Raper, O. F., Robbins, B. D., Toth, R. A., and Muller, C.: Simultaneous Spectroscopic Measurements of Stratospheric Species: O₃, CH₄, CO, CO₂, N₂O, H₂O, HCl, and HF at Northern and Southern Midlatitudes. *J. Geophys. Res.*, Vol. 85, 1980, pp. 1621-1632.
4. Morse, P. G.: Progress Report on the ATMOS Sensor: Design Description and Development Status. Paper No. 80-1914-CP, AIAA Sensor Systems for the 80's Conference, CP807, 1980.
5. Toon, G. C., Farmer, C. B., and Norton, R. H.: A Detection of Stratospheric N₂O₅ by Infrared Remote Sounding. *Nature*, in press.

TABLE 1. MAJOR CHARACTERISTICS OF THE ATMOS INSTRUMENT.

SPECTRAL INTERVAL COVERED	550-4800 cm^{-1} (2.1 TO 18 MICRONS)
SPECTRAL RESOLUTION	0.01 cm^{-1} UNAPODIZED (50 cm OPD)
SPECTRAL PRECISION	0.001 cm^{-1} (HE-NE REFERENCE LASER)
SPATIAL RESOLUTION	1 TO 2.5 Km
FIELD OF VIEW	1, 2, OR 4 MRAD, SELECTABLE
APERTURE	75 mm DIAMETER
SCANTIME	1 SECOND
POINTING ACCURACY	0.1 MRAD (2-AXIS SUNTRACKER)
DETECTOR	HgCdTe (77K)
DATA RATE	15.76 MEGABITS/SECOND
MASS	250 Kgm
VOLUME	~1 STERE (INCL. ELECTRONICS)
AVERAGE POWER	350 WATTS

TABLE 2. BANDPASSES OF THE PRIMARY ATMOS FILTERS WITH THE ATMOSPHERIC SPECIES WHICH ABSORB IN EACH REGION SHOWN. PARENTHESES INDICATE A SECONDARY REGION OF ABSORPTION FOR A GIVEN MOLECULE, WHOSE PRIMARY FEATURES LIE IN THE BANDPASS OF ANOTHER FILTER.

BAND 1 600-1200 cm^{-1}	BAND 2 1100-2000 cm^{-1}	BAND 3 1580-3400 cm^{-1}	BAND 4 3100-4700 cm^{-1}
CO_2	CO_2	CO_2	CO_2
H_2O	CH_4	CO	H_2O
O_3	H_2O	CH_4	
		H_2O	
		O_3	HF
NH_3		N_2O	(HCN)
HNO_2	H_2O_2		
(HNO_3)	HO_2		
HNO_4		NO	
	(NO)	(NO_2)	
CCl_3F	NO_2		
CCl_2F_2	N_2O_5	HDO	
CH_3CClF_2	HNO_3	(H_2O_2)	
CH_3Cl		H_2CO	
CCl_4	HOCl		
COF_2	CF_4	HCl	
COCIF		(CH_3Cl)	
ClO	SO_2		
ClONO_2		OCS	
		HCN	

TABLE 3. SUMMARY OF THE OCCULTATIONS OBTAINED BY ATMOS ON SPACELAB 3 LISTED BY MISSION ELAPSED TIME (MET), GEOGRAPHICAL LOCATION, AND OPTICAL FILTER NUMBER. SR DENOTES A SUNRISE OCCULTATION AND SS A SUNSET.

START TIME (MET)	OCC TYPE	OPT FIL	START LAT	START LON (E)
00/07:13	SR01	3	-50.10	118.25
00/08:08	SS01	1	36.87	277.60
00/18:52	SS02	1	36.18	117.31
00/19:27	SR02	3	-49.12	294.55
00/21:55	SS03	2	34.53	70.68
01/00:55	SS04	4	35.82	25.69
01/01:34	SR03	6	-49.10	203.09
01/02:28	SS05	1	34.80	2.26
01/07:01	SS06	3	32.90	292.66
01/08:33	SS07	2	33.65	270.20
01/10:05	SS08	1	33.73	247.39
01/15:18	SR04	4	-47.28	355.90
01/16:49	SR05	2	-47.80	333.43
01/18:21	SR06	1	-47.15	310.09
01/19:53	SR07	5	-46.97	287.07
02/01:22	SS09	3	29.95	16.84
02/02:53	SS10	4	30.28	354.13
02/04:25	SS11	3	29.00	330.65
02/05:51	SS12	2	28.65	307.61
02/07:27	SS13	3	29.65	285.23

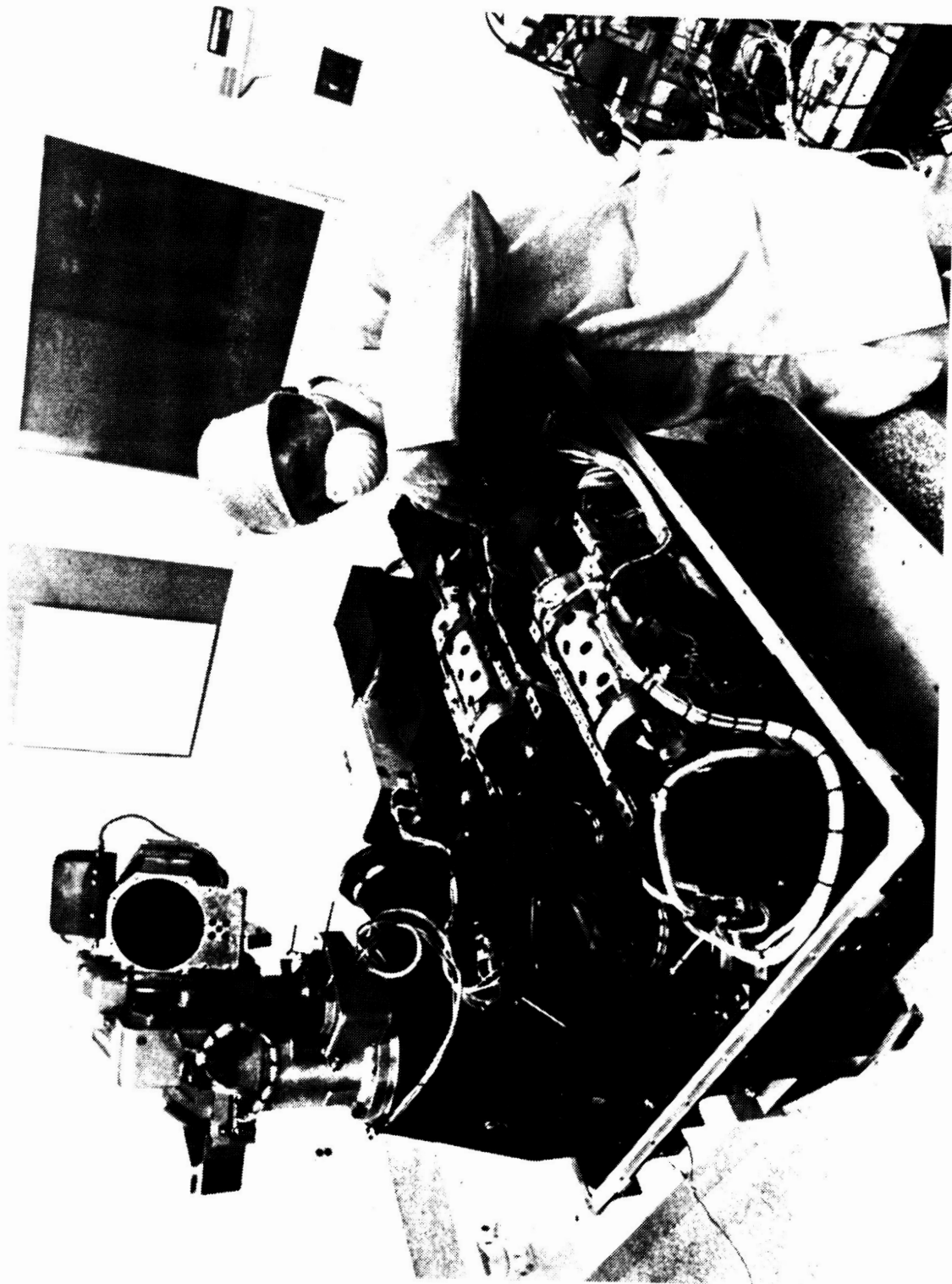


Figure 1. A cover-off photograph of the ATMOS instrument taken during the manufacturing phase at the Honeywell Electro-Optical Center. Prominent features are the two-axis suntracker seen in the upper left corner, the KBr beamsplitter and compensator and the retro mirror in the left center, and the large metal cylinders and drive motors containing the cat's-eyes.

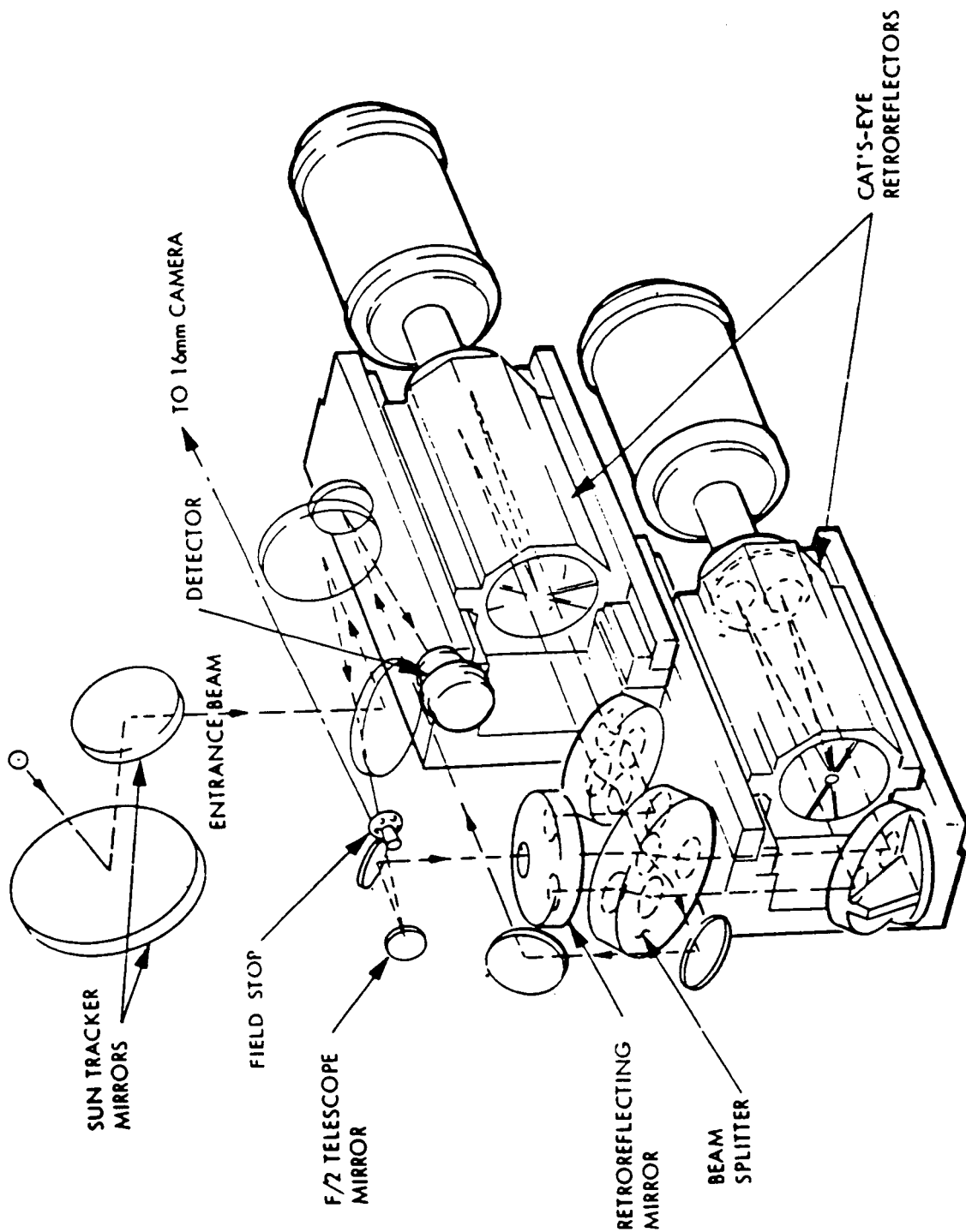


Figure 2. An optical diagram of the ATMOS sensor. Light enters through the two-axis suntracker and is focused via a telescope on a selectable field stop which defines the instrument's FOV. Light rejected by the field stop is redirected to a frame camera which records an image of the solar disk at the end of each scan. The field stop appears in the image as a black spot superimposed on the solar disk. Once inside the interferometer, the light is divided into two beams at the beamsplitter and transmitted to the two separate cat's-eyes. After each beam traverses its arm of the interferometer, the two are recombined at the beamsplitter and focussed on the HgCdTe detector.

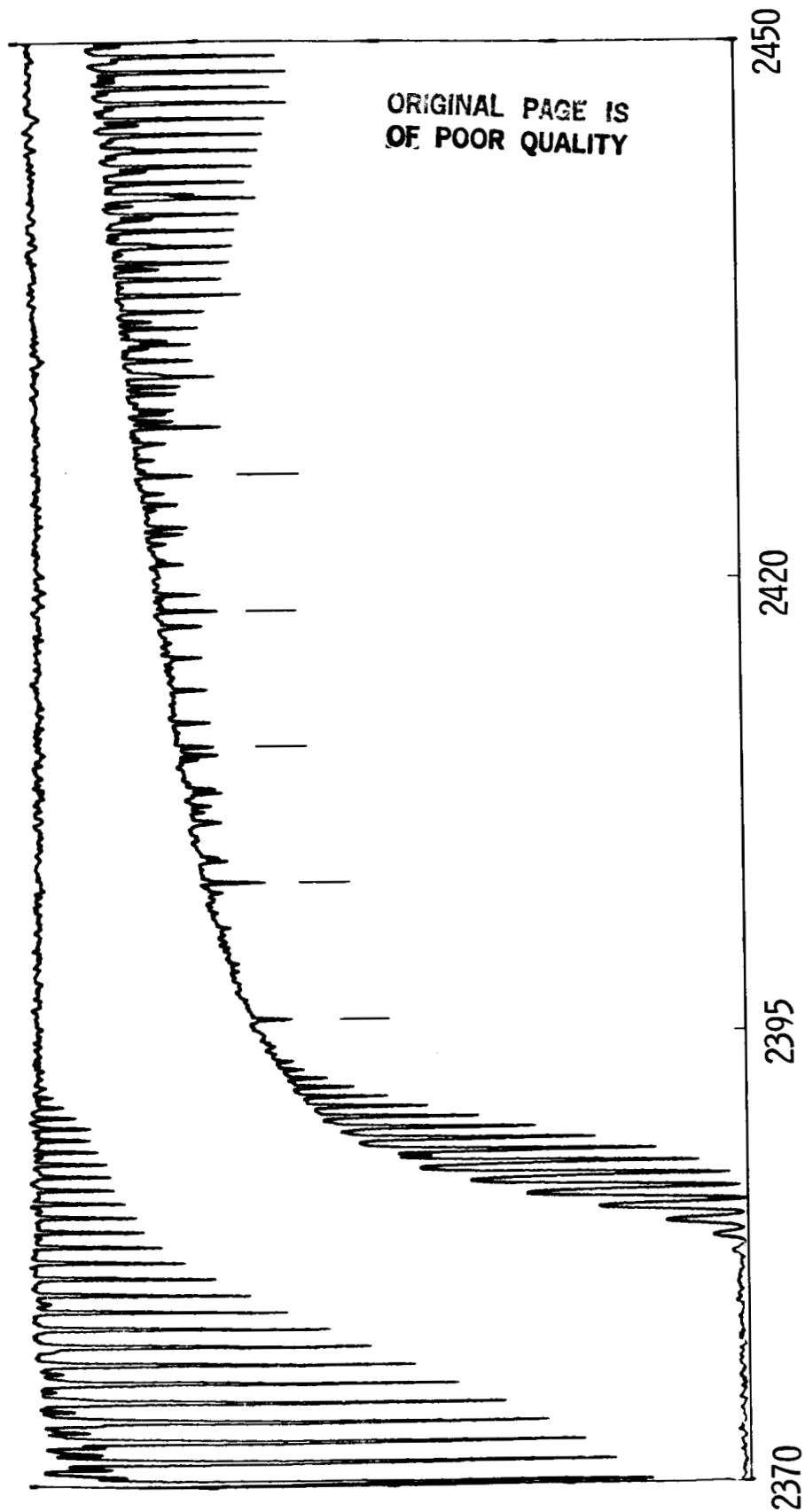


Figure 3. Two spectral excerpts shown in the temperature-sensitive high-J region of the ν_3 band of CO_2 and the pressure-induced absorption region for N_2 . The depression of the continuum in the lower trace is due to the diffuse pressure-induced dipole absorption of N_2 . The features marked by the vertical lines are the temperature-insensitive N_2 quadrupole lines used for density retrievals (identified from left to right as the S7 through S11 lines). Note that in the upper trace no absorption due to N_2 can be seen, even though N_2 is still the dominant gas in the region. This demonstrates the weak nature of both the dipole and quadrupole absorptions.

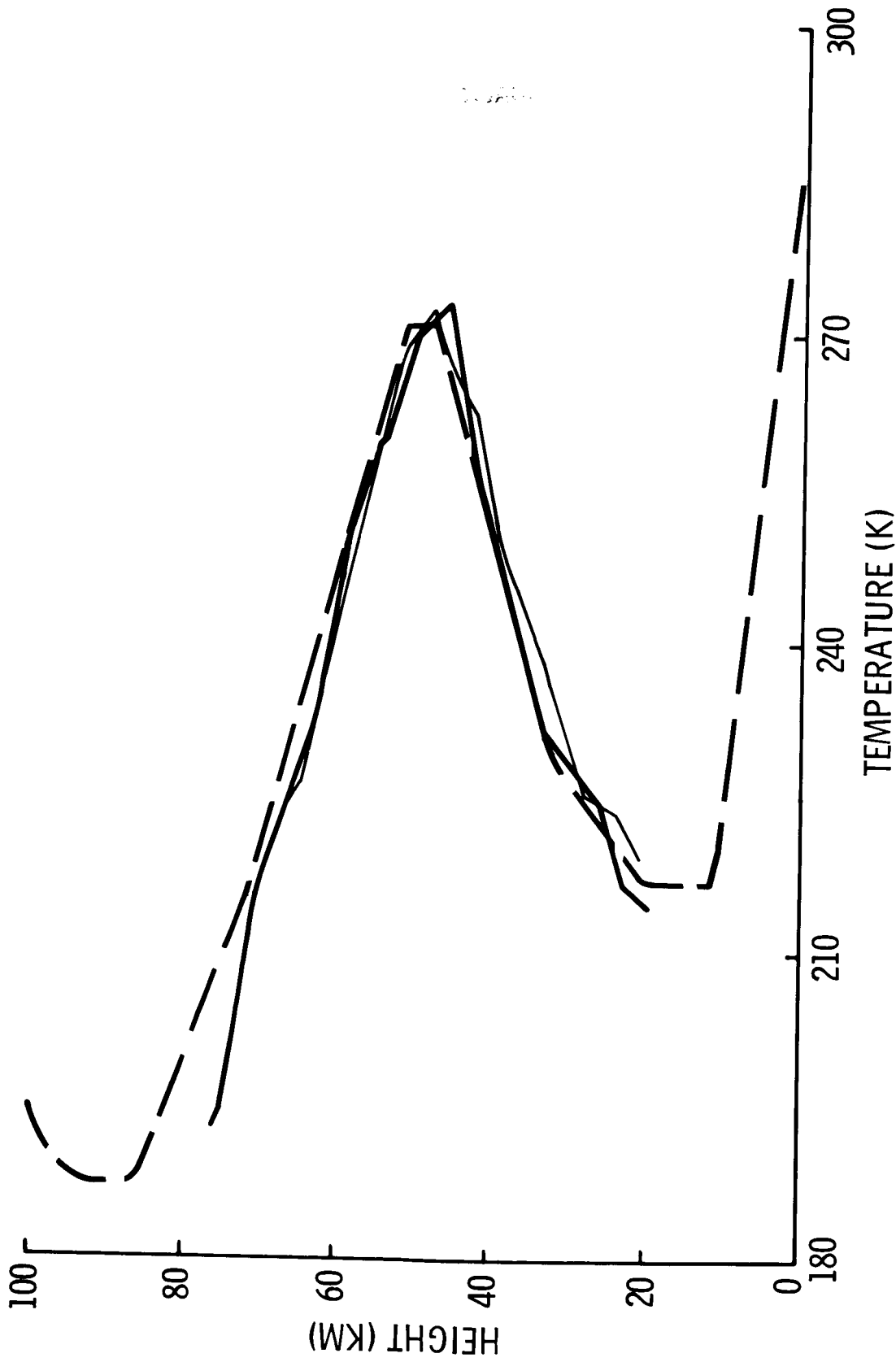


Figure 4. Two representative temperature-pressure profiles of the atmosphere derived from two ATMOS sunset observations by the method described in the text. The derived profiles (solid lines) are compared to the U.S. Standard Atmosphere for reference. Three other groups of ATMOS coinvestigators, using independent retrieval algorithms, have arrived at closely similar results for these occultations.

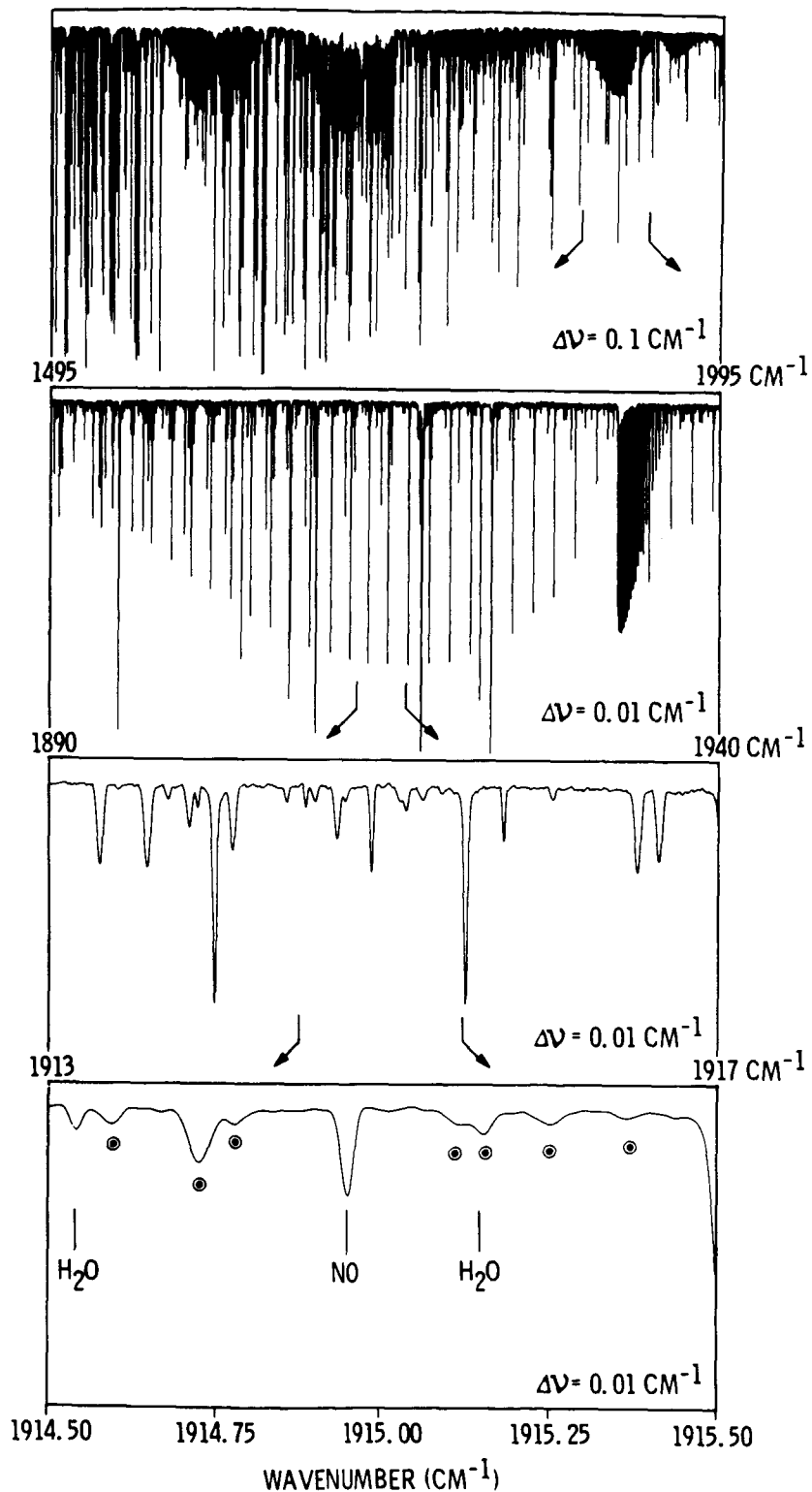


Figure 5. The top trace in this figure shows a 500 cm^{-1} region of spectrum between 1495 and 1995 cm^{-1} recorded with Filter 2. The second trace shows an expanded view of the 1900 to 1950 cm^{-1} region from the first, the third 4 cm^{-1} similar expanded from the second in the 1913 to 1917 cm^{-1} region, and finally 1 cm^{-1} expanded from the third trace centered on 1915 cm^{-1} . This one wavenumber region represents one of the selected microwindows for NO.

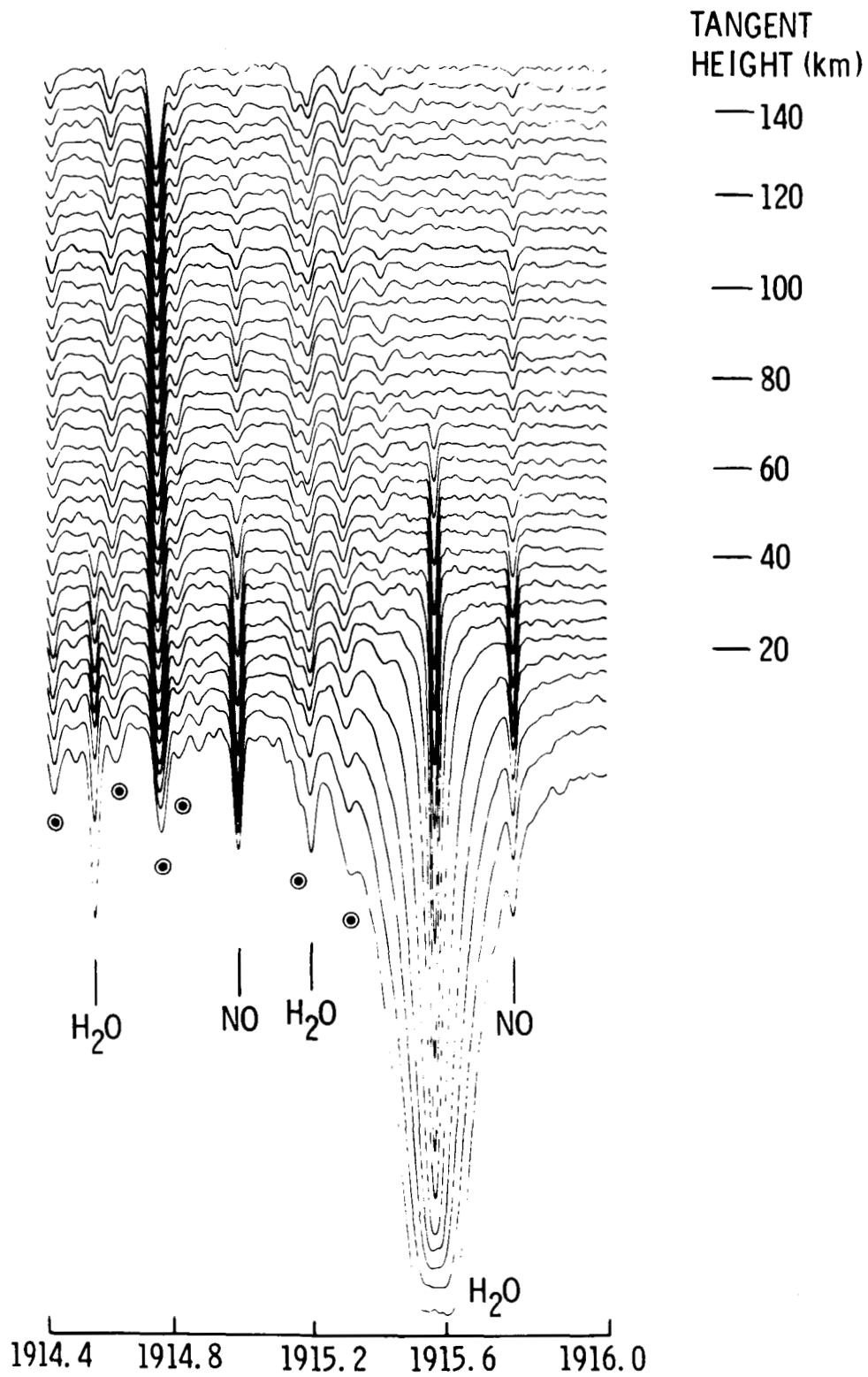


Figure 6. Shown in this figure are an entire set of 1.5 cm^{-1} spectral excerpts approximating the NO microwindow shown in Figure 5. For the purpose of clarity, the spectra have been overlaid as a function of altitude. Several other solar lines and lines of telluric origin are also present in the window, in addition to the two lines for NO at 1914.99 and 1915.77 cm^{-1} .

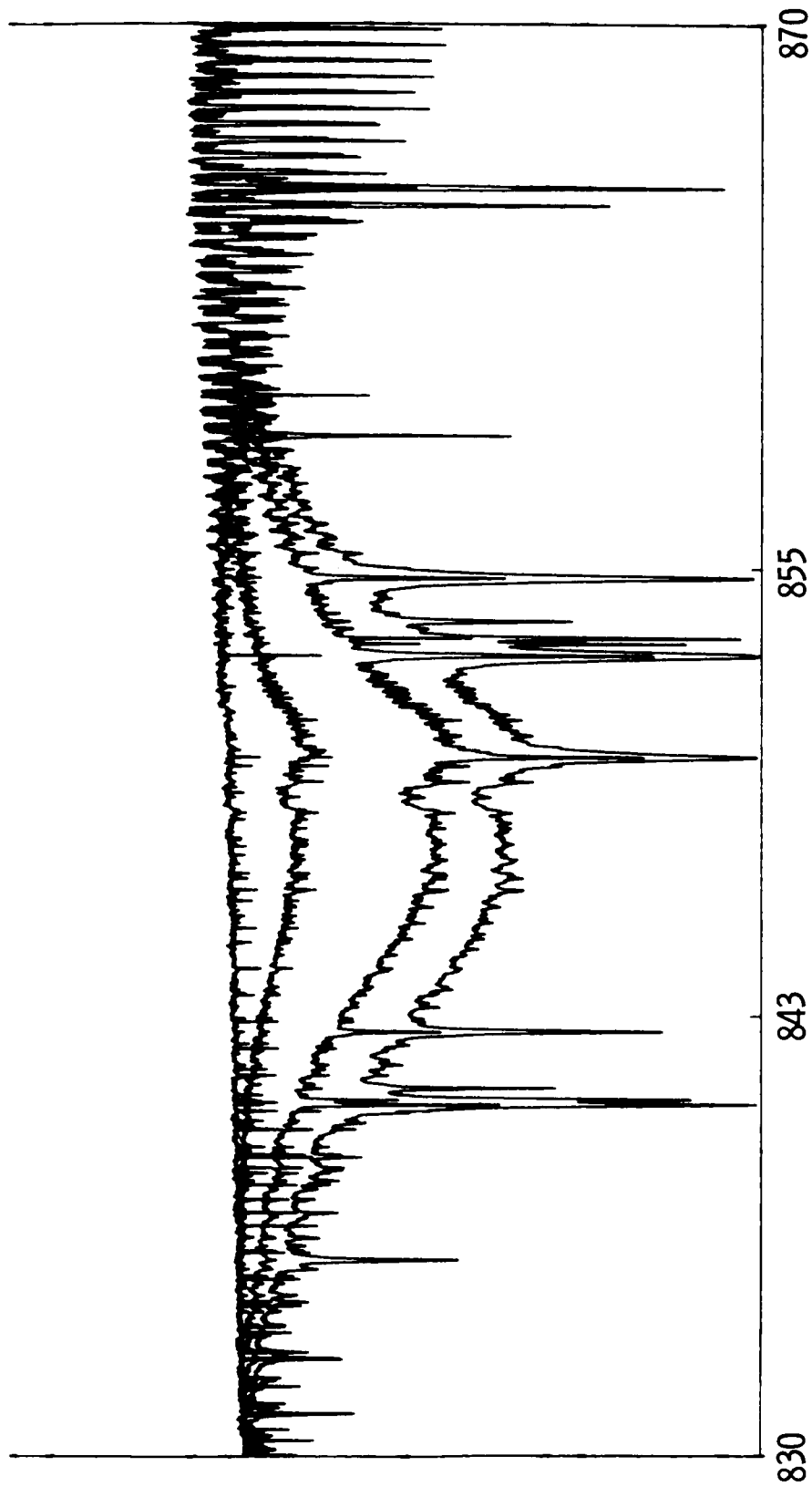


Figure 7. Portions of four spectra in the region of 830 to 870 cm^{-1} showing a large unresolved spectral feature of Freon 11 (F-11) in the lower three traces. The lowermost trace in the figure was made at 5 km altitude, and demonstrates that useful tropospheric information can be acquired using this remote sensing technique when atmospheric conditions are favorable. Such conditions prevailed for many of the ATMOS occultations.

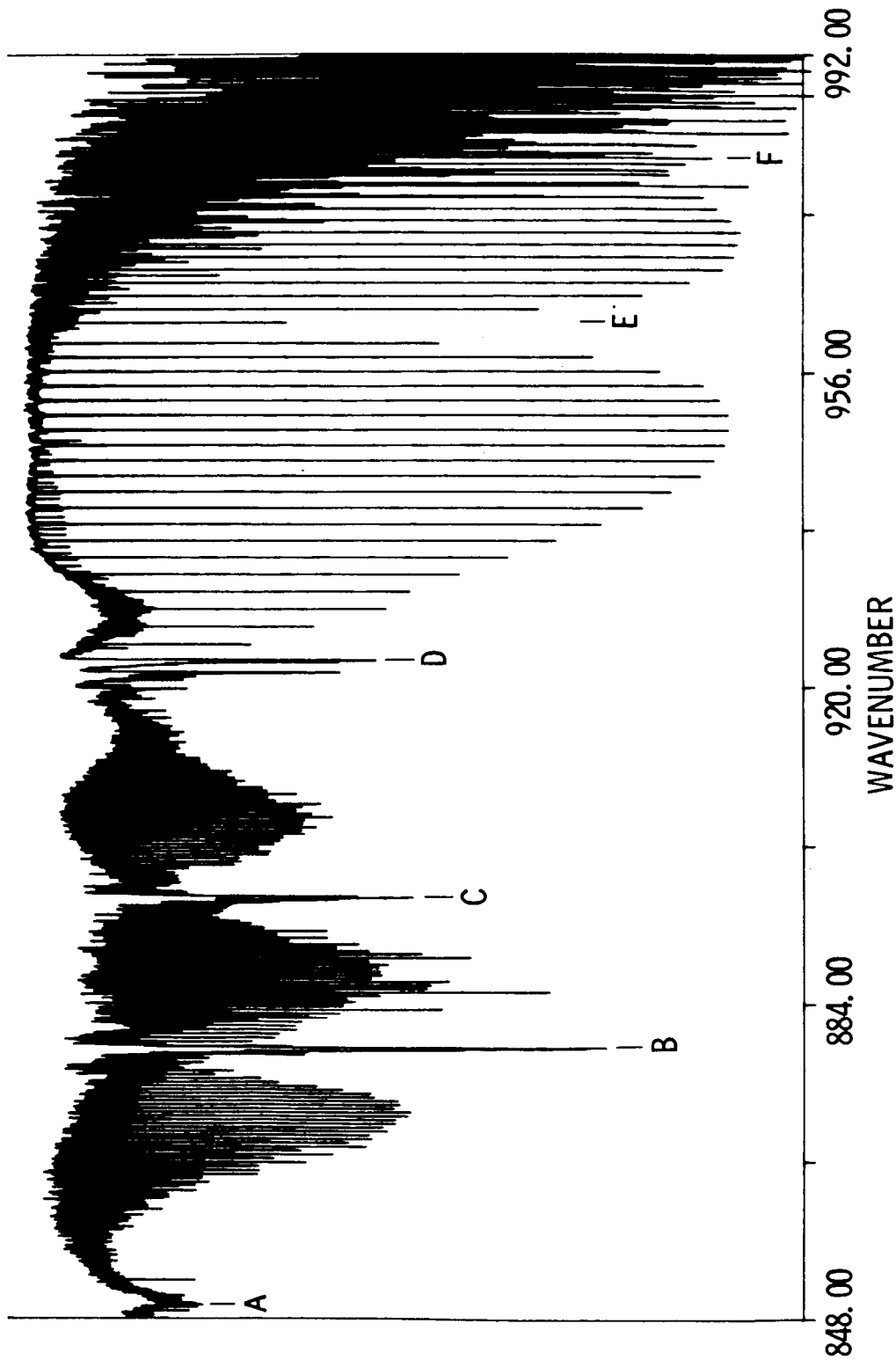


Figure 8. This figure demonstrates that dramatic asthetic effects in nature are not limited to the visible regions but rather occur throughout the electromagnetic spectrum. The feature marked by A in the figure is that of F-11 shown in Figure 6. The features whose Q branches are marked by B and C, respectively, are two transitions of HNO_3 ; the region between B and C is characterized by perturbations and blendings between the R branch lines of one feature and the P branch lines of the other. D marks the Q-branch of an F-12 absorption feature whose rotational lines are so densely packed they are completely unresolved at the ATMOS resolution, resulting in P and R branches which appear only as depressions in the continuum. E marks the center of a CO_2 absorption characterized by deep, relatively widely spaced rotational lines. Beyond F, tightly packed, seemingly chaotic lines of ozone begin to dominate the spectrum.

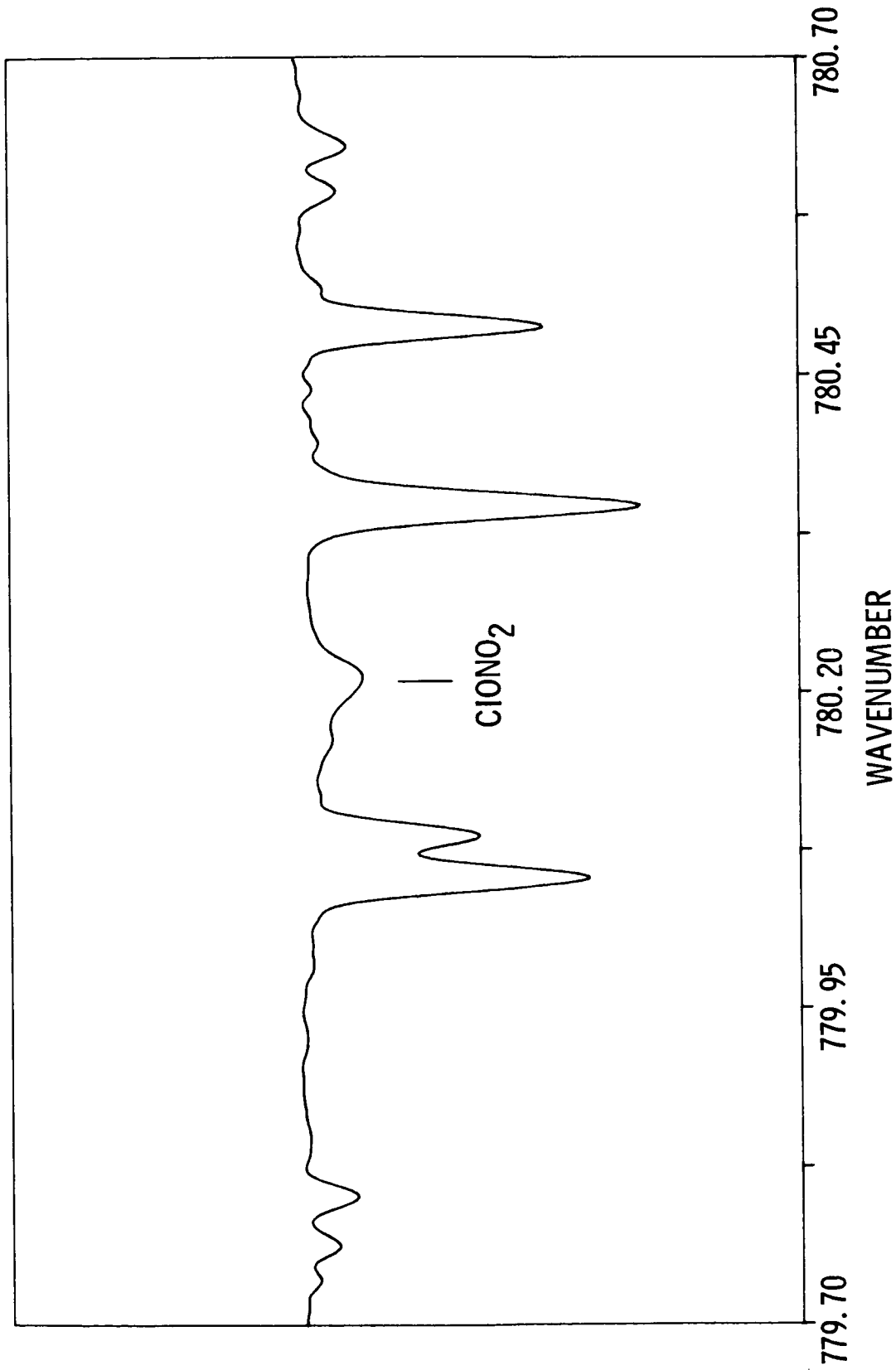


Figure 9. A portion of an ATMOS spectrum showing the feature of ClONO_2 at 780.22 cm^{-1} . This figure illustrates one of the marked advantages of acquiring spectra in large sets such as that returned from SpaceLab 3. The spectrum shown, as well as the others used in retrieving the ClONO_2 profile, are zonal averages of several spectra from occultations in the same latitudinal regions using the same optical filter and covering the same altitude range. Such averaging can enhance the signal-to-noise characteristics, causing otherwise marginal features to stand out in the data and permit profiles of concentration to be obtained at only minimum costs in spatial resolution.

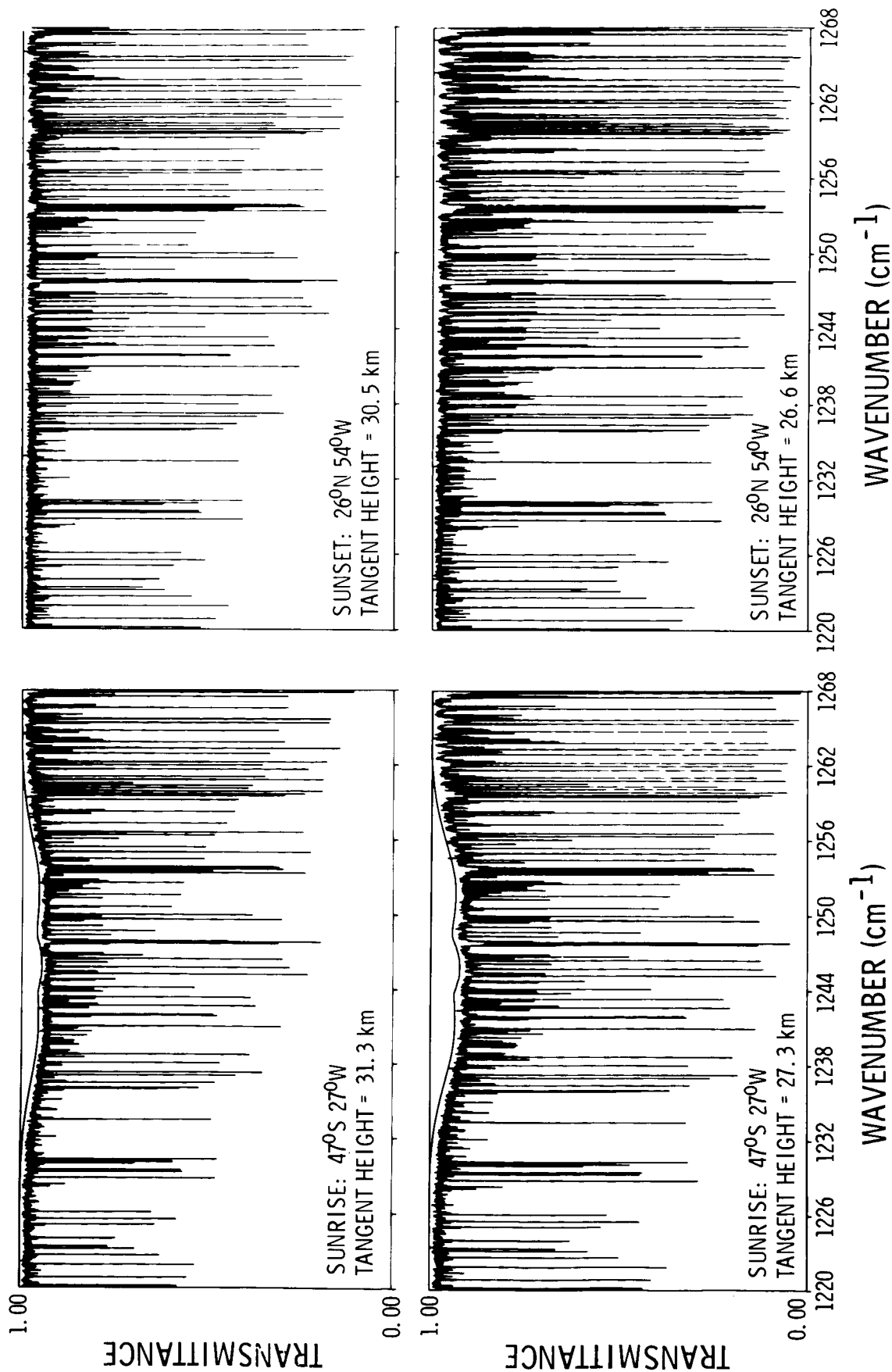


Figure 10. This figure, reprinted from Toon, C. G., et al., (1986) shows the ν_{12} band of N_2O_5 in the ATMOS spectra. The solid lines above the sunrise spectra in the figure represent a spectroscopic model of the ν_{12} feature, the lines of which are completely unresolved at the ATMOS resolution. The figure clearly illustrates the sunrise-sunset difference in the N_2O_5 profiles as predicted by the photochemical models.

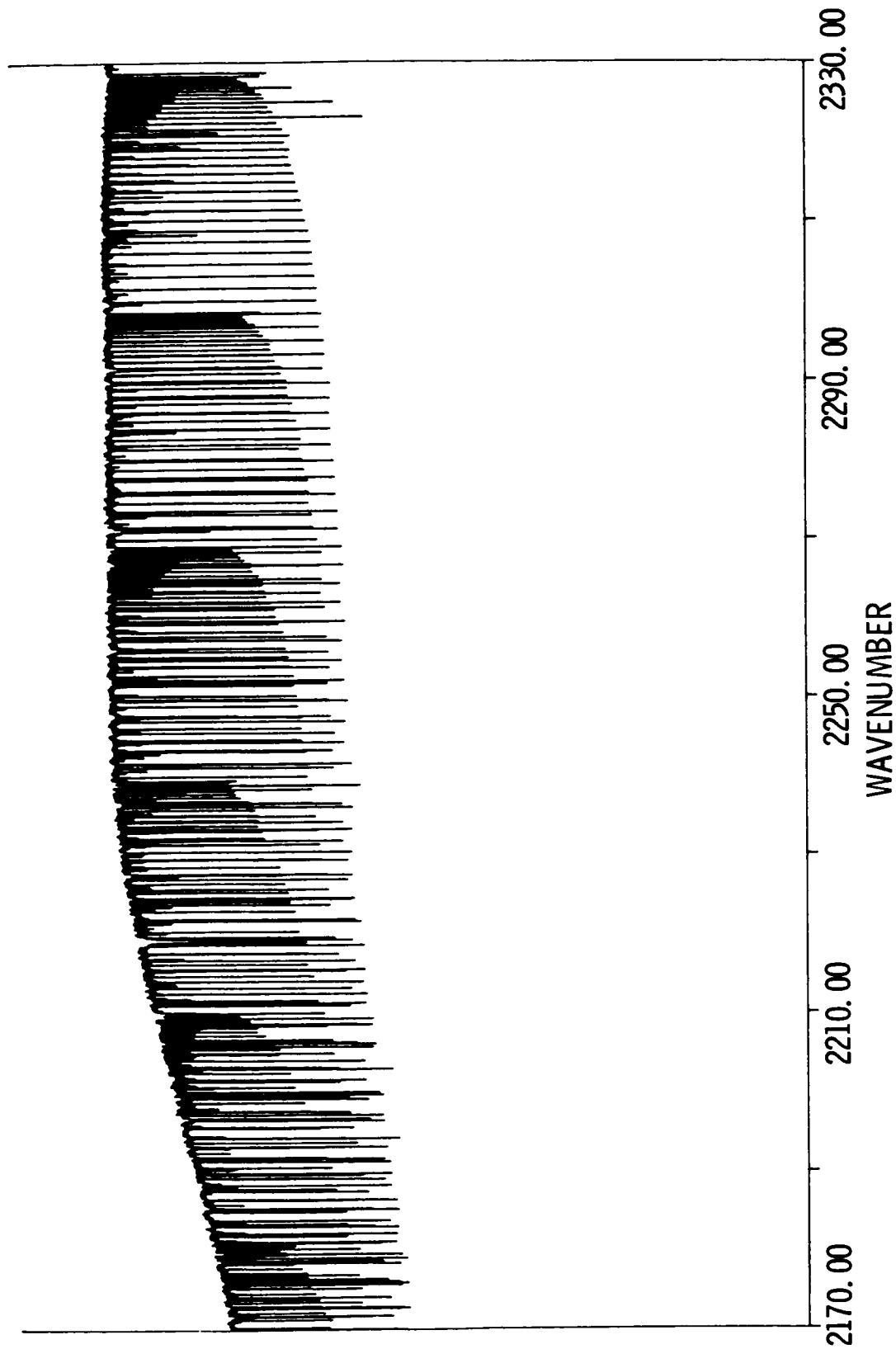


Figure 11. The outstanding features in this figure are the band heads resulting from transitions between the higher vibrational states of CO with $\nu = 1$. These features are not seen in telluric spectra, but are solar in nature and occur in the photosphere of the Sun as a result of the high temperatures present in the region. Note the classical folding back of the lines in the band heads at the higher values of J.

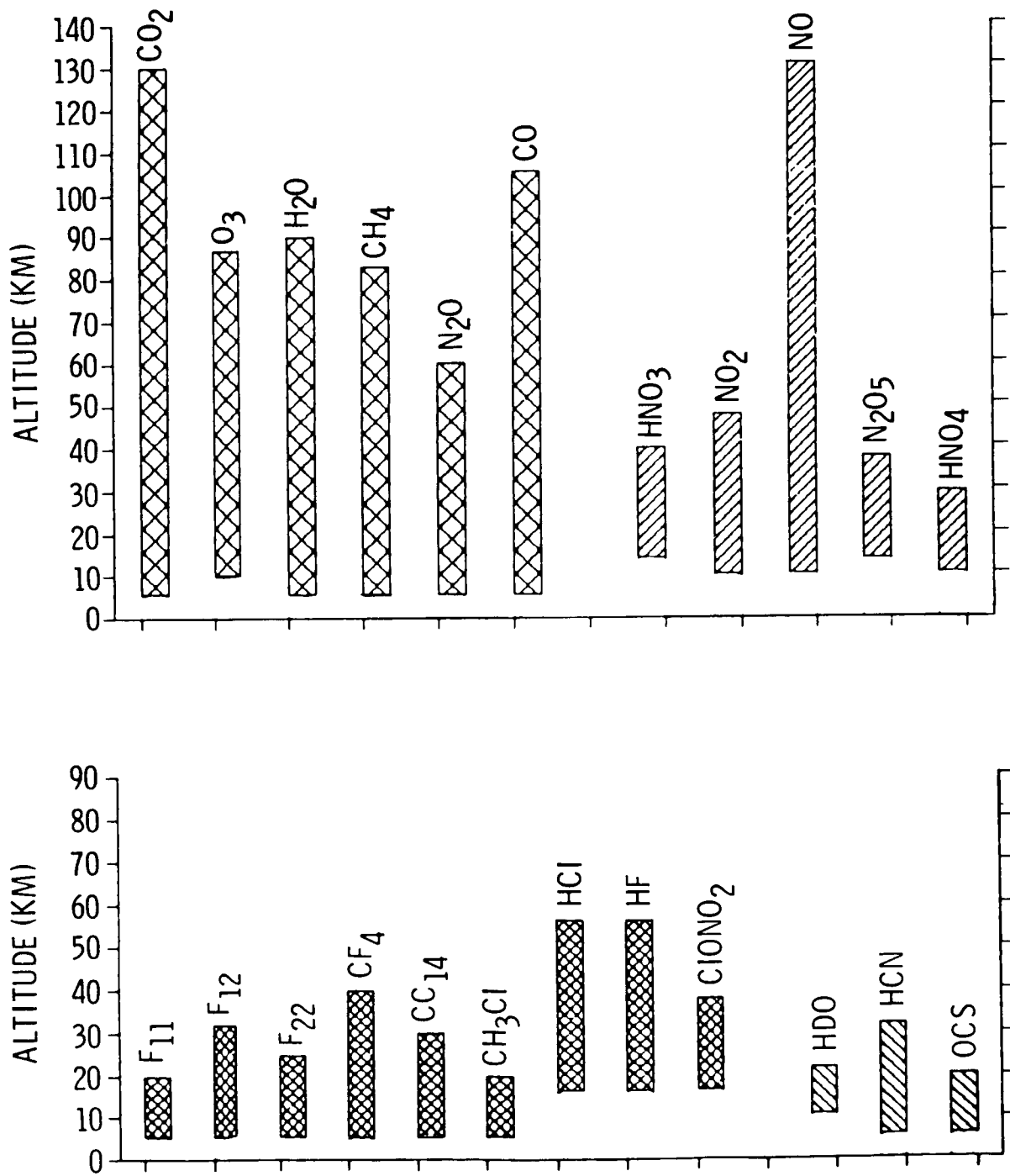


Figure 12. Diagrammatic summary of species detected in the ATMOS spectra, separated into the minor gases and chemical families of trace species; the bars indicate the altitude ranges over which profiles of concentration can be retrieved from the data.